



Cite this: *React. Chem. Eng.*, 2022, 7, 2280

Received 3rd August 2022,
Accepted 23rd September 2022

DOI: 10.1039/d2re00310d

rsc.li/reaction-engineering

The upscaling of biphasic photochemical reactions is challenging because of the inherent constraints of liquid–gas mixing and light penetration. Using semi-permeable coaxial flow chemistry within a modular photoreactor, the photooxidation of the platform chemical furfural was scaled up to produce routinely 29 gram per day of biobased building block hydroxybutenolide, a precursor to acrylate alternatives.

Photooxygenation^{1,2} has become a staple synthetic tool for a wide range of application-oriented processes including photodynamic therapy,^{3,4} wastewater treatment,⁵ late-stage functionalization,⁶ drug synthesis⁷ and monomer preparation,^{8,9} due to the sustainable, mild but also selective nature of the oxidant singlet oxygen (${}^1\text{O}_2$).¹⁰ Paired with the low cost¹¹ and opportunities for large-scale production¹² of platform chemicals, the photooxidation towards biobased building blocks is an exceptionally attractive and environmentally benign method in line with the principles of green chemistry.¹³ When aiming at industrial production, it is highly important to show applicability of these transformations on a larger scale, which brings serious physical limitations to batch processes, *e.g.* mass transfer of oxygen or light penetration. In sharp contrast, performing photooxidation reactions in flow offers significant advantages over traditional batch photooxidation reactions, overcoming these constraints without compromising safety.^{14,15} Over the years the field of photooxidation reactions in flow has evolved, starting from the most straightforward method of segmented flow^{16,17} towards advanced falling film,^{18,19} vortex,^{20,21} spinning disk,²² ultrasonic,²³ solar

concentrator,^{24,25} membrane^{26,27} and coaxial (a.k.a. “tube-in-tube”)^{28–31} designs with improved productivities, shorter reaction times and allowing operation at higher concentrations. Yet, shifting a working batch process to a continuous one remains tedious, and often requires the assembly of a completely new setup (a new light source with a specific wavelength, tubing, heating element, cooling system,

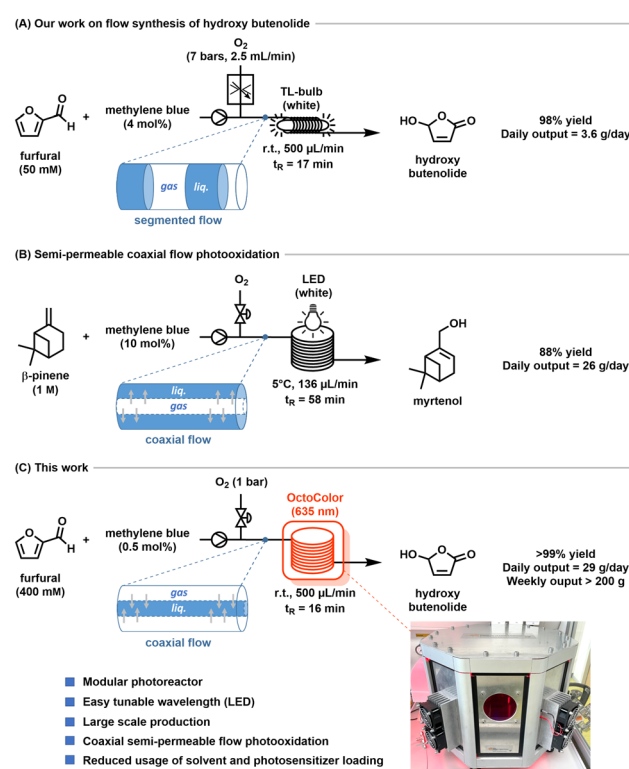


Fig. 1 A. Our segmented flow design for the photooxidation of furfural. B. Previously described coaxial flow design for the photooxidation of β -pinene; with liquid phase on outside. C. Coaxial flow photooxidation of furfural using the modular photoreactor OctoColor; with liquid phase on inside for convenience.

^a Stratingh Institute for Chemistry, Advanced Research Center Chemical Building Blocks Consortium (ARC CBC), University of Groningen, Nijenborgh 4, 9747 AG Groningen, The Netherlands. E-mail: b.l.feringa@rug.nl

^b Hanze University of Applied Sciences, Zernikeplein 11, 9747 AS Groningen, The Netherlands

† Electronic supplementary information (ESI) available. See DOI: <https://doi.org/10.1039/d2re00310d>



compatible pumps and gas supply, *etc.*), which can be prohibitively expensive and not transferable to another transformation. Furthermore, optimization after assembly may reveal design flaws that would soon render obsolete in the newly built setup. A modular photoreactor that would generally allow the optimization and scale-up of photooxidations (or any photochemical process involving a gas phase) is thus highly desired.

In recent studies, we have shown that hydroxybutenolide, the product of the photooxidation of the platform chemical furfural, can be used as a precursor for the synthesis of valuable monomers (maleic anhydride and acrylic acid),⁹ or for the production of sustainable acrylate alternatives for biobased coatings.⁸ We reported the continuous production of this building block *via* the photooxidation of furfural in segmented flow in transparent fluorinated ethylene propylene (FEP) tubing, which was coiled around an 18 W TL-bulb as the light source (Fig. 1A).⁸ Under the optimized conditions, a maximum productivity of 1.5 mmol h^{-1} (less than 4 g per day) was reached, with 98% conversion towards hydroxybutenolide. The productivity of the reaction could be further scaled up to 7.5 mmol h^{-1} by using a numbering-up strategy of five setups in parallel,^{32,33} but the overall design proved sub-optimal (poor cooling, low concentration, high catalyst loading).

To the best of our knowledge, only one example of semi-permeable coaxial flow photooxidation of platform chemicals has been reported (Fig. 1B).²⁸ In this work, Park *et al.* demonstrated the major improvement in productivity of myrtenol upon successively changing from batch to segmented flow to coaxial flow using 10 mol% photosensitizer. Natural sunlight could also be used as the light source instead of the original white light LED setup, albeit with a lower overall conversion. Although continuous flow microreactors facilitate light penetration, it is highly important to capitalize on matching the emission spectrum of the light source with the absorption spectrum of the photosensitizer in order to reach the highest productivity.

Here, we report the development of a benchtop modular photoreactor (OctoColor) that can be used for the upscaling and optimization of photochemical reactions in flow. We also provide (in the ESI†) the corresponding detailed technical manual for equipment replication. A notable feature of the modular photoreactor is that the wavelength of the irradiation can be changed effortlessly by simply swapping the aluminum plates carrying the LEDs due to the slide-in-slide-out design (Fig. 2). Besides, the reactor can be assembled using inexpensive and widely available components (see the ESI† Construction Manual OctoColor). The upscaled continuous photooxidation of furfural (Fig. 1C) served as a benchmark of this semi-permeable coaxial flow reactor and resulted in a greatly increased productivity (8-fold) compared to our previous design based on standard segmented flow, while simultaneously drastically decreasing the solvent and catalyst (0.5 mol%) usage 8-fold.

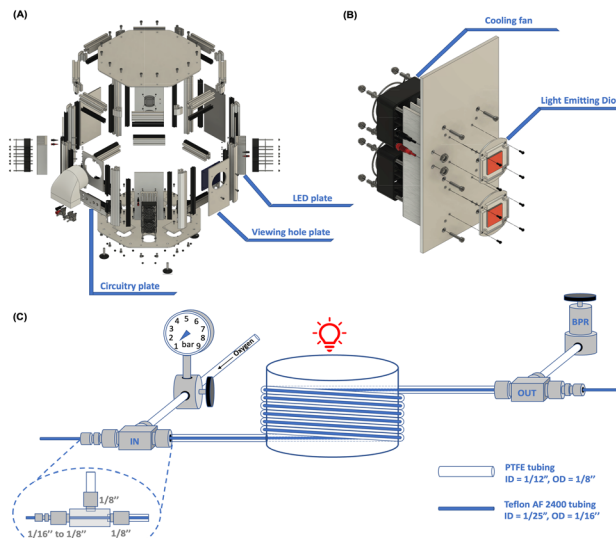


Fig. 2 A. Schematic exploded view of OctoColor reactor. B. Schematic exploded view of LED plate. For details of construction, see SI OctoColor construction manual. C. Schematic representation of a coaxial flow reactor.

The OctoColor reactor described in this study was built as an octagon (Fig. 2A–C) such that a coil of tubing placed inside would be irradiated from all sides. The reactor itself consists of eight removable aluminum plates, four of which are carrying two 50 W LEDs, for a total of eight LEDs and maximum 400 W power. Both red and blue LED plates have been assembled to demonstrate the modularity of the system. The emission spectrum of the red and blue plates can be found in the ESI† (Fig. S8 and S10). Every LED is individually cooled by a 1.6 W fan, and four additional fans located on the bottom plate are dedicated to cooling the reactor's chamber. With all LEDs on (200 W, half of the maximum power), room temperature could be maintained indefinitely inside the reactor. One side-plate displays a viewing hole (stained to filter the wavelength in use), while another one is equipped with an outlet for air and circuitry. The aluminum plates are held together by aluminum struts with rubber side guides in an angle of 135° and are easily removable by sliding. Although not used, the two remaining aluminum plates could be customized with extra LEDs. A detailed building manual for replication of the photoreactor is provided in the ESI† (Construction Manual OctoColor).

As part of our program towards sustainable photocatalytic oxidation, the further upscaling of hydroxybutenolide production was of great interest. It was decided to improve the existing segmented flow system by developing a new reactor based on coaxial flow chemistry. A coaxial flow setup (colloquially called “tube-in-tube”) consists of a gas-permeable inner tube (Teflon AF 2400, an amorphous fluoropolymer)³⁴ inserted in a standard non-permeable Teflon-based outer tube. Teflon AF2400 has a >300 times higher oxygen permeability than commonly used fluoropolymers such as PFA and PTFE.³⁵ This assembly



allows for a large contact interface (50 cm^2 per meter of tubing with $\text{ID} = 1 \text{ mm}$) between a liquid and a gas phase along the length of the reactor.³⁶ As shown by Ley and coworkers, a better flow is generally obtained when the inner tube is used for the liquid phase while the outer tube is the shell for the pressurized bulk of gas.³⁷ The lack of absorbance of fluoropolymers in the visible range guarantees efficient light penetration, even to the inner tubing. For our studies, a 12 meter Teflon AF-2400 ($\text{ID} = 1/25'' = 1.0 \text{ mm}$, $\text{OD} = 1/16'' = 1.6 \text{ mm}$) inner tubing and a 10 meter regular FEP outer tubing ($\text{ID} = 1/12'' = 2.1 \text{ mm}$, $\text{OD} = 1/8'' = 3.2 \text{ mm}$) were used (Fig. 2C). Ten meters of the double tubing was coiled around a plastic cylinder ($\mathcal{O} = 16 \text{ cm}$) and placed in the middle of the OctoColor. The outer tubing was connected to an oxygen cylinder with pressure reducer and to a closed back pressure regulator to ensure a constant pressurized oxygen atmosphere in the outer tube (Fig. 2C). The inner tube was connected to a Vapourtech SF 10 peristaltic pump. A detailed description of installing the coaxial tube is provided in the ESI† (page S4 and S5). For the photooxidation of furfural, utilizing methylene blue as the photosensitizer, we aimed to use the red ($\lambda_{\text{max}} = 635 \text{ nm}$) LED plates. We first tested our original segmented flow setup ($\text{IV} = 49.5 \text{ mL}$) to determine whether the OctoColor would have a constructive impact on the productivity. A brief optimization already increased the productivity by a factor 4 (Table S1†), mostly by allowing either a higher flow rate or a higher concentration. This first step nicely exemplifies the potential of the OctoColor for the optimization of photochemical processes in flow.

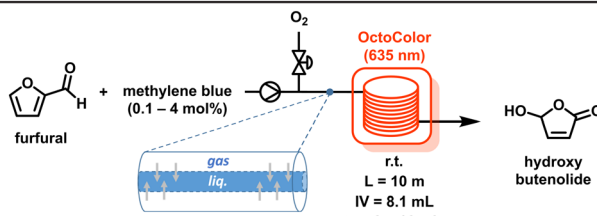
Using the coaxial semi-permeable flow setup ($\text{IV} = 8.1 \text{ mL}$), we started with the conditions optimized for the previous segmented flow system, *i.e.* a 0.2 M solution of

furfural in methanol with 4 mol% methylene blue at a 0.5 mL min^{-1} flow rate and 7 bar of oxygen. To our delight, full conversion towards the desired hydroxybutenolide was achieved (Table 1, entry 1).

However, we noticed that the residence time of the reaction mixture was very short ($\approx 90 \text{ s}$) and did not scale with flow rate, presumably due to the large overpressure of oxygen causing liquid/gas phase separation on the length of the tubing. Lowering the pressure of oxygen to 1 bar suppressed the phase separation and thus significantly increased the residence time to its expected value ($\approx 16 \text{ min}$ for a reactor volume of 8.1 mL and flow rate of 0.5 mL min^{-1}). Although less oxygen was entering the inner tube, full conversion towards the desired hydroxybutenolide was maintained, suggesting an efficient mass transfer to the liquid phase (Table 1, entry 2). It is important to note that coaxial reactors passively provide continuous feeding of oxygen, allowing lower working pressures and therefore enhancing general safety.³¹

With the incentive of upscaling, it is essential to obtain optimized conditions with high concentrations of substrate. Studying the concentration of furfural showed an upper limit of 0.4 M to reach full conversion (Table 1, entries 3–5). As the amount of oxygen could be the limiting reagent, the pressure of oxygen was increased to 2 bar, while keeping a 0.4 M concentration of furfural. This resulted however in a lower conversion, supposedly due to the decreased residence time (Table 1, entries 6–7), arising from liquid/gas phase separation. In order to establish the importance of the residence time, the flow rate was altered between 1 and 4 mL min^{-1} . A significant decrease in conversion demonstrated the

Table 1 Optimization of continuous coaxial flow photooxidation of furfural towards hydroxybutenolide



Entry	Conc. furfural (M)	Cat. loading (mol%)	Flow rate ^b (mL min ⁻¹)	Press. O ₂ (bar)	Yield ^a (%)	Productivity (mmol h ⁻¹)
1	0.2	4	0.5	7	>99	6.0
2	0.2	4	0.5	1	>99	6.0
3	0.4	4	0.5	1	>99	12.0
4	0.5	4	0.5	1	70	10.5
5	0.6	4	0.5	1	63	11.3
6	0.4	4	0.5	2	53	6.4
7	0.6	4	0.5	2	21	3.8
8	0.4	4	1.0	1	82	19.7
9	0.4	4	2.0	1	51	24.5
10	0.4	4	4.0	1	33	31.7
11	0.4	0.5	0.5	1	>99	12.0
12	0.4	0.1	0.5	1	94	11.3
13	0.4	0	0.5	1	0	0

^a Yield determined by ¹H-NMR spectroscopy in CDCl_3 based on the ratio of substrate and product integrals. ^b Residence time (t_R) can be calculated by dividing internal volume ($\text{IV} = 8.1 \text{ mL}$) by the flow rate of solution.



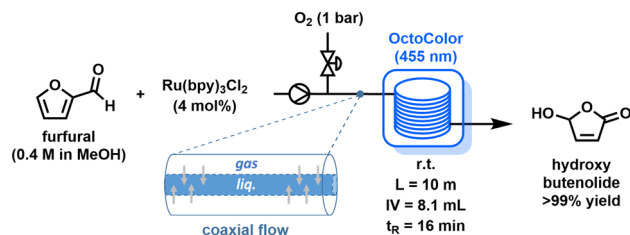


Fig. 3 Photooxidation of furfural towards hydroxybutenolide using $\text{Ru}(\text{bpy})_3\text{Cl}_2$ as photosensitizer. OctoColor arranged with blue LED plates. Reaction conditions in coaxial semi-permeable flow: 0.4 M furfural in methanol, $\text{Ru}(\text{bpy})_3\text{Cl}_2$ (4 mol%), rt, oxygen, 455 nm, 8.1 mL internal volume.

limit of the productivity was reached for this length of tubing (Table 1, entries 8–10, Fig. S11†). Although at higher flow rates full conversion towards hydroxybutenolide was not achieved, a higher productivity was still observed (Fig. S11†). It is important to emphasize that, regarding large scale production of a building block, full conversion is warranted as no subsequent purification steps are required, *i.e.* hydroxybutenolide can be used as is for further condensations. If desired, the product can also be isolated through filtration and recrystallization with 60% yield (ESI† pages S10 and S11).⁸ Finally, the photosensitizer loading was reduced to 0.5 mol% without impacting conversion, showing the effectiveness of the singlet oxygen formation under flow conditions (Table 1, entries 11–12). As expected, the photooxidation is unsuccessful in the absence of a photosensitizer (Table 1, entry 13). Under our optimal conditions (Table 1, entry 11: 0.4 M furfural, 0.5 mol% methylene blue, 0.5 mL min^{−1} flow rate, 1 bar O₂) the continuous production resulted in 29 g per day (>200 g per week) in which selective and high-yielding transformation (>99%) of furfural to hydroxybutenolide was achieved (Fig. S6 and S7, S12 and S13†).

We also verified that the intensity of light provided by the red LEDs is optimal (ESI† pages S14 and S15). With the current price of electricity (€0.33 per kW h),³⁸ the production of 1 kg of hydroxybutenolide costs €60.14 over 35 days. This compares very favourably to our previous segmented-flow design,⁸ for which the same production would cost €39.59 over more than 9 months: productivity is increased 8-fold for an energy input of the same order of magnitude. Besides, the use of solvent and photosensitizer are also reduced 8-fold, whereas the working oxygen pressure has been significantly decreased. Altogether, the OctoColor reactor allowed us to greatly and quickly improve the performance of the photooxygenation of furfural on multiple aspects.

To further demonstrate the modularity of the system, the red LED plates were exchanged for blue LED plates and $\text{Ru}(\text{bpy})_3\text{Cl}_2$ was used as a blue light activated photosensitizer.³⁹ Under the near-optimal conditions described in entry 3 of Table 1, furfural was selectively and quantitatively transformed to hydroxybutenolide (Fig. 3).

In conclusion, a novel modular photochemical reactor was developed that can be used in particular for continuous flow photochemical reactions. This setup allows for irradiation from all sides while the lamps can be easily exchanged due to the slide-in-slide-out design of the aluminum plates if other wavelengths are required as was shown using distinct photosensitizers. A detailed manual for the replication of this reactor has been provided.

The photochemical reactor was used in combination with a semi-permeable coaxial flow design in order to upscale the photooxidation of the platform chemical furfural towards the bio-based building block hydroxybutenolide with a productivity of 29 g per day (200 g per week) in quantitative conversion with full selectivity. An asset to this design is the inherent safety it presents as these gas/liquid reactions, especially photooxidations with singlet oxygen, can be performed at low working pressures and in small volumes. This system shows that large quantities can be produced in a mild, selective and straightforward method, strengthening the viability of photooxidation reactions for the development of sustainable building blocks.

Author contributions

B. L. F. and E. K. conceptualized and coordinated the research project. A. K., R. B. and M. M. built the photochemical reactor. J. G. H. H., M. L. L., R. B. and M. M. conducted the research and its validation. J. G. H. H., M. L. L., A. K. and B. L. F. prepared the manuscript with input from E. K. All authors reviewed the manuscript.

We thank K. J. van den Berg and N. Elders from AkzoNobel Coatings BV for fruitful discussion and suggestions. Funding: this work is part of the Advanced Research Center for Chemical Building Blocks, ARC CBBC, which is cofounded and cofinanced by The Netherlands Organization for Scientific Research (NWO, contract 736.000.000) and The Netherlands Ministry of Economic Affairs and Climate.

Conflicts of interest

There are no conflicts to declare.

Notes and references

- 1 C. S. Foote and E. L. Clennan, in *Active Oxygen Chemistry*, ed. C. S. Foote, J. S. Valentine, A. Greenberg and J. F. Lieberman, Springer Netherlands, Dordrecht, 1995, ch. Properties and Reactions of Singlet Dioxygen, pp. 105–140.
- 2 B. König, in *Chemical Photocatalysis*, ed. B. König, De Gruyter, Berlin, Boston, 2013, pp. 45–61.
- 3 M. Riethmüller, N. Burger and G. Bauer, *Redox Biol.*, 2015, **6**, 157–168.
- 4 J. F. Algorri, M. Ochoa, P. Roldán-Varona, L. Rodríguez-Cobo and J. M. López-Higuera, *Cancers*, 2021, **13**, 4447.
- 5 D. García-Fresnadillo, *ChemPhotoChem*, 2018, **2**, 512–534.
- 6 T. Montagnon, D. Kalaitzakis, M. Triantafyllakis, M. Stratakis and G. Vassilikogiannakis, *Chem. Commun.*, 2014, **50**, 15480–15498.



7 A. A. Ghogare and A. Greer, *Chem. Rev.*, 2016, **116**, 9994–10034.

8 J. G. H. Hermens, T. Freese, K. J. V. D. Berg, R. V. Gemert and B. L. Feringa, *Sci. Adv.*, 2020, **6**, eabe0026.

9 J. G. H. Hermens, A. Jensma and B. L. Feringa, *Angew. Chem., Int. Ed.*, 2022, **61**, e202112618.

10 I. Pibiri, S. Buscemi, A. Palumbo Piccione and A. Pace, *ChemPhotoChem*, 2018, **2**, 535–547.

11 S. H. Krishna, K. Huang, K. J. Barnett, J. He, C. T. Maravelias, J. A. Dumesic, G. W. Huber, M. de Bruyn and B. M. Weckhuysen, *AIChE J.*, 2018, **64**, 1910–1922.

12 S. Takkellapati, T. Li and M. A. Gonzalez, *Clean Technol. Environ. Policy*, 2018, **20**, 1615–1630.

13 P. T. Anastas and J. C. Warner, *Green Chemistry: Theory and Practice*, Oxford University Press, 1998.

14 S. V. Ley, *Chem. Rec.*, 2012, **12**, 378–390.

15 C. Sambiagio and T. Noël, *Trends Chem.*, 2020, **2**, 92–106.

16 B. D. A. Hook, W. Dohle, P. R. Hirst, M. Pickworth, M. B. Berry and K. I. Booker-Milburn, *J. Org. Chem.*, 2005, **70**, 7558–7564.

17 F. Lévesque and P. H. Seeberger, *Org. Lett.*, 2011, **13**, 5008–5011.

18 T. H. Rehm, S. Gros, P. Löb and A. Renken, *React. Chem. Eng.*, 2016, **1**, 636–648.

19 O. Shvydkiv, K. Jähnisch, N. Steinfeldt, A. Yavorskyy and M. Oelgemöller, *Catal. Today*, 2018, **308**, 102–118.

20 D. S. Lee, Z. Amara, C. A. Clark, Z. Xu, B. Kakimpa, H. P. Morvan, S. J. Pickering, M. Poliakoff and M. W. George, *Org. Process Res. Dev.*, 2017, **21**, 1042–1050.

21 D. S. Lee, M. Sharabi, R. Jefferson-Loveday, S. J. Pickering, M. Poliakoff and M. W. George, *Org. Process Res. Dev.*, 2020, **24**, 201–206.

22 A. Chaudhuri, K. P. L. Kuijpers, R. B. J. Hendrix, P. Shivaprasad, J. A. Hacking, E. A. C. Emanuelsson, T. Noël and J. van der Schaaf, *Chem. Eng. J.*, 2020, **400**, 125875.

23 Z. Dong, S. D. A. Zondag, M. Schmid, Z. Wen and T. Noël, *Chem. Eng. J.*, 2022, **428**, 130968.

24 D. Cambié, J. Dobbelaar, P. Riente, J. Vanderspikken, C. Shen, P. H. Seeberger, K. Gilmore, M. G. Debije and T. Noël, *Angew. Chem., Int. Ed.*, 2019, **58**, 14374–14378.

25 S. D. A. Zondag, T. M. Masson, M. G. Debije and T. Noël, *Photochem. Photobiol. Sci.*, 2022, **21**, 705–717.

26 R. A. Maurya, C. P. Park and D.-P. Kim, *Beilstein J. Org. Chem.*, 2011, **7**, 1158–1163.

27 C. P. Park, R. A. Maurya, J. H. Lee and D.-P. Kim, *Lab Chip*, 2011, **11**, 1941–1945.

28 C. Y. Park, Y. J. Kim, H. J. Lim, J. H. Park, M. J. Kim, S. W. Seo and C. P. Park, *RSC Adv.*, 2015, **5**, 4233–4237.

29 L. Yang and K. F. Jensen, *Org. Process Res. Dev.*, 2013, **17**, 927–933.

30 M. B. Plutschack, B. Pieber, K. Gilmore and P. H. Seeberger, *Chem. Rev.*, 2017, **117**, 11796–11893.

31 S. Han, M. A. Kashfipour, M. Ramezani and M. Abolhasani, *Chem. Commun.*, 2020, **56**, 10593–10606.

32 Y. Su, K. Kuijpers, V. Hessel and T. Noël, *React. Chem. Eng.*, 2016, **1**, 73–81.

33 J. Zhang, K. Wang, A. R. Teixeira, K. F. Jensen and G. Luo, *Annu. Rev. Chem. Biomol. Eng.*, 2017, **8**, 285–305.

34 I. Pinna and L. G. Toy, *J. Membr. Sci.*, 1996, **109**, 125–133.

35 J. F. Greene, Y. Preger, S. S. Stahl and T. W. Root, *Org. Process Res. Dev.*, 2015, **19**, 858–864.

36 M. Brzozowski, M. O'Brien, S. V. Ley and A. Polyzos, *Acc. Chem. Res.*, 2015, **48**, 349–362.

37 T. P. Petersen, A. Polyzos, M. O'Brien, T. Ulven, I. R. Baxendale and S. V. Ley, *ChemSusChem*, 2012, **5**, 274–277.

38 Average energy prices for consumers, <https://www.cbs.nl/en-gb/figures/detail/84672ENG> (accessed on 2022/07/24).

39 E. K. Pefkianakis, D. Christodouleas, D. L. Giokas, K. Papadopoulos and G. C. Vougioukalakis, *Eur. J. Inorg. Chem.*, 2013, 4628–4635.

